RA Journal of Applied Research
ISSN (e): 2394-6709
||Volume||3||Issue||12||Pages-1270-1287||December-2017||
Index Copernicus ICV: 74.25, DOI: 10.18535/rajar/v3i12.04

Use of Atmospheric Modeling for Megacity Urban Planning: The Case of Temperature Positive Anomalies in the Rio de Janeiro Metropolitan Area, Brazil

Nilton Oliveira Moraes[1], Luiz Claudio Gomes Pimentel[2], Fernando Pereira Duda[3], Corbiniano Silva[4], William Cossich Marcial de Farias[5], Edilson Marton[6]

[1]Doctoral Fellow, Mechanical Engineering Program (PEM), Alberto Luiz Coimbra Institute of Post Graduate Studies and Research (COPPE), Federal University of Rio de Janeiro (UFRJ), Rio de Janeiro, Brazil.

[2,6]Associate Professor, Dept. of Meteorology, Federal University of Rio de Janeiro (UFRJ), Rio de Janeiro, Brazil.

[3]Associate Professor, Mechanical Engineering Program (PEM), Alberto Luiz Coimbra Institute of Post Graduate Studies and Research (COPPE), Federal University of Rio de Janeiro (UFRJ), Rio de Janeiro, Brazil.

[4]Postdoctoral Fellow, Faculty of Geology, Center for Technology and Sciences, State University of Rio de Janeiro (UERJ), Rio de Janeiro, Brazil.

[5]Substitute Professor, Dept. of Meteorology, Federal University of Rio de Janeiro (UFRJ), Rio de Janeiro, Brazil.

Corresponding Author: Nilton Oliveira Moraes

[1]Doctoral Fellow, Mechanical Engineering Program (PEM), Alberto Luiz Coimbra Institute of Post Graduate Studies and Research (COPPE), Federal University of Rio de Janeiro (UFRJ), Rio de Janeiro, Brazil.

Abstract: This study aims at the evaluation of the ability of the atmospheric mesoscale model of Weather Research and Forecasting (WRF) to predict heat wave episodes in the RMRJ, Brazil. The results obtained by using the WRF were compared with observed data of air temperature at 2 meters, showing a slight tendency of the simulated results to underestimate the observed temperatures. On the other hand, the results of the simulation adequately reproduced the daily temperature cycle. In the period of analysis, the observed data indicated values of maximum temperatures about 5 ° C above the climatological means of each sub-region of the RMRJ, which characterizes episodes of a heat wave. The synoptic analysis indicated that the temperature anomalies occurred as a consequence of the meteorological configuration in the synoptic scale of the ASAS in low levels and a high of geopotential in average levels of the troposphere. The study demonstrates that the meteorological characterization together with the computational modeling of the atmosphere is a potential strategy for urban planning and public management of urban areas, capable of detecting and predicting the area's most susceptible to the occurrence of positive temperature anomalies in Megacities.

keywords: Heat waves; Atmospheric modeling; Urban planning; Megacities; Rio de Janeiro; WRF; temperature positive anomalies .

RA Journal of Applied Research
ISSN (e): 2394-6709
||Volume||3||Issue||12||Pages-1270-1287||December-2017||
Index Copernicus ICV: 74.25, DOI: 10.18535/rajar/v3i12.04

Introduction

Perspectives on global urbanization point that 54% of the population live in urban areas, and this figure will reach 66% by 2050 (Grimm et al. 2008; Cleugh and Grimmond 2012; United Nations 2014; Baklanov et al. 2016). At the same time, the amount of urban lands has expanded at a rate twice the population growth (Angel et al. 2011) and is expected to triple by 2030 if current trends of population density remain the same (Seto et al. 2012).

As urbanization progresses, leveraged and accelerated mainly by factors related to economic growth and development of cities, various social, economic and environmental problems develop, geographic space planning, population health, among other consequences. Urbanization leads to processes of change in using and covering lands on a global scale, intensified by the growth of population and buildings, which triggered the expansion of urban areas on the countryside, farmland and vegetation, spaces converted into impervious surfaces of cement, asphalt and concrete (Quattrochi and Luvall 1997).

The world megacities, characterized by highly developed urban centers, producing the so-called Urban Heat Islands (UHI), a phenomenon identified by the higher temperatures under the influence of the same atmospheric conditions as temperatures observed in peripheral areas of large cities and contributing to intensify extreme temperature phenomena such as Heat Waves (HW), whose synergy (Li and Bou-Zeid 2013) favors the intensification of the difference between urban and rural temperatures, resulting in higher impacts related to heat in megacities.

In the literature, the most discussed impacts related to HW are the damage to public health. Many studies have linked the occurrence of high temperatures to the demand for specific medical treatments or medical emergencies (Hess et al. 2014; Tasian et al. 2014). The increase in human mortality rates is one of the main addressed issues (Semenza et al. 1996; Conti et al. 2005; Ostro et al. 2009; Hoshiko et al. 2010; Huang et al. 2010; Gasparrini and Armstrong 2011; Lim et al. 2012; Jongsik and Kim 2012; Monteiro et al. 2012). Other implications involve forest fires and air pollution episodes (Vautard et al. 2005), impacts on agriculture and terrestrial ecosystems (Ciais et al., 2005), and the shortage of energy (Fink et al. 2004).

In Brazil, which has a total of 70 metropolitan areas, HW is a social and environmental problem, related to urban planning and, especially, public health in many of these areas, including the Greater Rio de Janeiro (RMRJ), a space whose urban area is highly dense, mainly due to the explosive and widespread urbanization in the twentieth century, driven by industrialization.

Currently 12.3 million inhabitants (IBGE 2016) live in RMRJ, which is the largest urban area on the Brazilian coast and brings together the second largest industrial complex in Brazil. The industrialization process in this area, driven by metal and steel and logistical and oil industries and chained with other industries and their associated activities, is included in the economic restructuring of the state of Rio de Janeiro, occupying and expanding in different areas on a regional scale, especially in RMRJ with the creation of new productive territories, with emphasis on the Petrochemical Complex of Rio de Janeiro (COMPERJ) and the companies of Sepetiba Bay: Porto de Itaguaí, TKCSA, Gerdau, Usiminas, Petrobras, LLX, among others (Chagas 2015); spaces integrated into airshed III, Guanabara Bay region which houses the largest industrial occupation of the state, with developments of the Industrial Hub of Campos Elíseos, in Duque de Caxias, petrochemical

RA Journal of Applied Research
ISSN (e): 2394-6709
||Volume||3||Issue||12||Pages-1270-1287||December-2017||
Index Copernicus ICV: 74.25, DOI: 10.18535/rajar/v3i12.04

industries, manufacturing and power plants, especially Duque de Caxias Refinery (REDUC).

The main advances on the topic HW in metropolitan areas use meteorological models whose physical parameterizations represent urban areas with direct effects on the estimates of the heat balance, momentum and water surface, capable of reproducing the effects of such structures in the urban microclimate (Chen et al. 2011; Chen and Dudhia 2001a, 2001b). Rizwan et al. (2008) emphasized that these models are very important and are currently essential for the study of heat transport, especially the simulation of heat transfer processes in the surface-atmosphere interface. The mesoscale models, with emphasis on the Weather Research and Forecasting (WRF), are more detailed than the global models and have been adopted in the study of UHI's and HW in various metropolitan areas in the world (Moraes et al. 2014; Lin et al. 2008; Dandou et al. 2009; Chemel and Shoki 2012; Kusaka et al. 2012; Salamanca et al. 2012; Miao et al. 2009; Chen et al. 2011; Li and Bou-Zeid 2013; Chen et al. 2011, 2014; Stéfanon et al. 2014 and Bittencourt et al. 2016).

Conceptualizing the importance of atmospheric modeling for the study of HW and the potential of meteorological models for the representation of atmospheric transport mechanisms of heat, moisture and momentum, even in regions with complex land and under the combined action of weather systems different spatial and temporal scales, the first objective of the research is to evaluate the ability of WRF atmospheric model for the representation of heat transfer mechanisms in the atmosphere and numerical prediction of the occurrence of HW in RMRJ. A second goal involves a brief discussion of the synoptic configuration that enhances positive anomalies of air temperature in RMRJ and possible episodes of HW.

Materials and Methods

Study Area

RMRJ (Figure 1) is bounded to the south (S) by the Atlantic Ocean and to the North (N) with the mountainous regions of Serra da Mantiqueira and Serra dos Órgãos whose elevations exceed 2000m. Guanabara Bay is located in the eastern portion and the Sepetiba Bay is located in the western border, as well as lakes and ponds distributed throughout the region. Inside there are areas of marshland, areas with altitudes around 1000 m, such as the massifs of Tijuca, Pedra Branca and Gericinó-Mendanha, as well as areas of urban forest, such as Tijuca Forest. Given this geographical complexity and the need for atmospheric studies and air quality in the region, RMRJ is divided into Air Basin (AB), sub-regions bordering the similarity of pollutant dispersion and atmospheric circulation mechanisms in surface (Paiva et al. 2014), as outlined in Figure 1, which also shows the surface meteorological stations (Table 1).

RA Journal of Applied Research
ISSN (e): 2394-6709
||Volume||3||Issue||12||Pages-1270-1287||December-2017||
Index Copernicus ICV: 74.25, DOI: 10.18535/rajar/v3i12.04

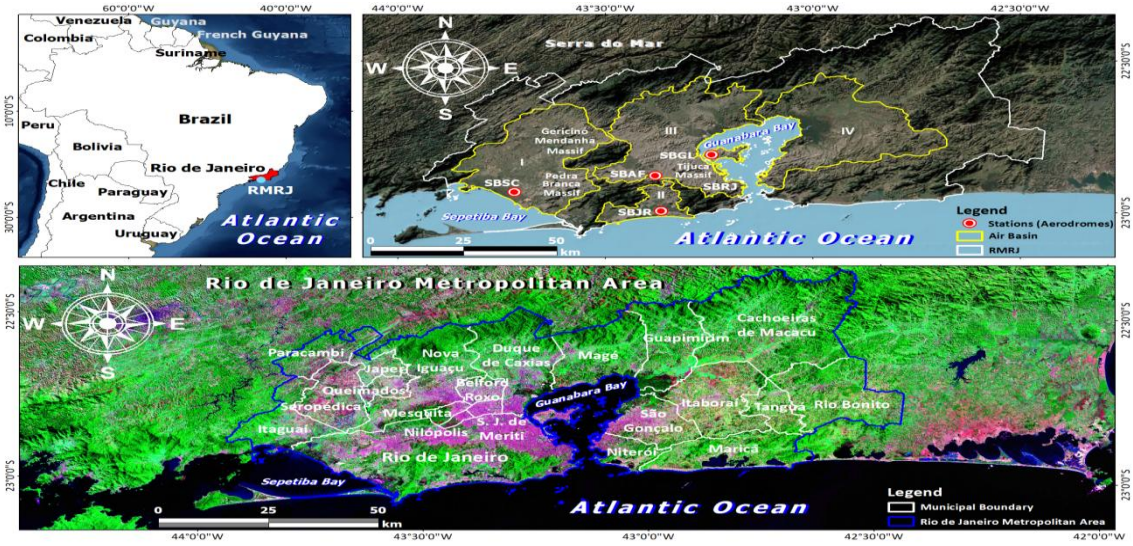

Fig. 1. Study Area Geographic location.

Table 1. Location of stations (aerodromes) and their Air Basins.

Stations (Aerodromes) And Air Basins (AB)	Location	
	Latitude	Longitude
Galeão (SBGL) / AB III	22° 48' S	43° 15'W
Santos Dumont (SBRJ) /	22° 54' S	43° 10 W
Afonsos (SBAF) / AB III	22° 52' S	43° 23' W
Jacarepaguá (SBJR) / AB II	22° 59' S	43° 22' W
Santa Cruz (SBSC) / AB I	22° 56' S	43° 43' W

Description and configuration of the WRF model (Weather Research and Forecasting)

Prognosis atmospheric model WRF - ARW is a state-of-the-art numerical weather prediction model, with physical and mathematical formulation for the simulation of atmospheric flow in compressible and non-hydrostatic conditions, developed both for research and operational purposes. The model code is open and is designed to be flexible, portable and efficient in parallel computing environments. It offers a variety of physical parameterizations, and advanced data assimilation systems that are being developed and tested along with the model. It can be used in applications of different spatial scales, from hundreds of meters to thousands of kilometers. Further details of the features and capabilities of WRF are available in http://www.wrf-model.org/index.php and Shamarock et al. (2008).

WRF was initialized with meteorological data from global model GFS (Global Forecast System), NCEP (National Centers for Environment Prediction) and assimilated with a spatial resolution of 0.5° and temporal resolution of 3 hours. This database provides the initial and boundary conditions of WRF.

In the simulations for the study area, we used 4 domains (Figure 2), the first being the most comprehensive and of lower spatial resolution and the other three nested with horizontal spatial resolution, decreasing at the ratio of 3: 1 (Table 2) using two-way interaction between the fields and allowing consider the interactions between the processes of the synoptic scale, mesoscale and microscale (Shafran et al, 2000). All domains have been configured with 43 sigma levels in the vertical. In these areas, soil use and cover and topography data from the USGS (United States Geological Survey) database were used, in the preprocessing module of the WRF, according to different spatial resolutions and according to

RA Journal of Applied Research
ISSN (e): 2394-6709
||Volume||3||Issue||12||Pages-1270-1287||December-2017||
Index Copernicus ICV: 74.25, DOI: 10.18535/rajar/v3i12.04

Table 2. After the initial configuration of WRF, physical parameterizations were chosen (Table 3), addressing the physical processes of sub-grade, from the prognostic variables that enter the dynamic equations of WRF.

Table 2. Characteristics of each domain used in the simulations

Domains	Characteristics			
	Points in x and y	Horizontal resolution (km)	Dimension of the grid - (°) (Latitude/Longitude)	Topography /LULC USGS (km)
1	36 x 36	27	-27.9855 - 17.6476 -49.0136 - 37.7028	19
2	46 x 46	9	-24.878 - 20.6618 -45.5574 - 41.0169	9
3	76 x 76	3	-23.8487 - 21.6731 -44.4406 - 42.0757	1
4	160 x 160	1	-23.1840 - 22.7186 -44.0435 - 42.4624	1

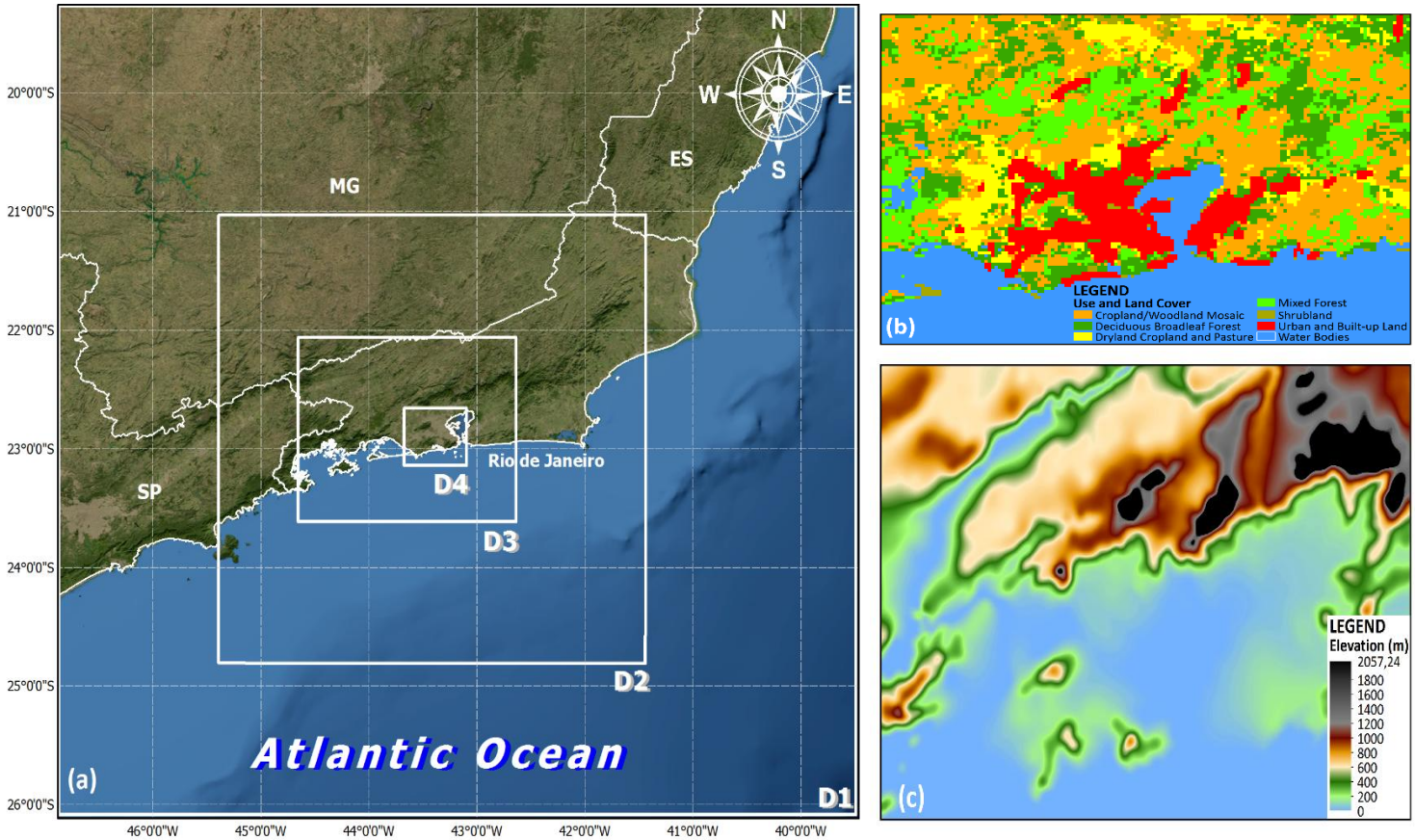

Fig. 2. Domains simulated by WRF (a), Use and land cover (b) and Topography (c), both in domain 4.

RA Journal of Applied Research
ISSN (e): 2394-6709
||Volume||3||Issue||12||Pages-1270-1287||December-2017||
Index Copernicus ICV: 74.25, DOI: 10.18535/rajar/v3i12.04

Table 3. Parameterization used in the simulations with WRF.

Physical Parameter	Reference
Cumulus	Grell (1993)
Cloud	Dudhia (1989)
Shortwave	Dudhia (1989)
Long-wave	Dudhia (1989)
Soil	NOAH LSM Soil Model (Chen e
Atmospheric	Mellor e Yamada (1974, 1982)
Surface Layer	Janjic (1996, 2002)

Study and Evaluation Period of the results of WRF model

The evaluation of the WRF results is based on qualitative and statistical criteria, in the period from January 20th to January 26th, 2014, to assess the performance of the model to represent the expected physical behaviors and present a satisfactory agreement with the times observed regularly at weather stations located at aerodromes in the METAR code form (METeorological Aerodrome Report). These stations belong to the network of stations of the World Meteorological Organization (WMO) and meet the calibration and maintenance procedures required by such organization and the aviation, in which it is believed that they provide reliable data for the assessment of WRF of the above-mentioned airsheds.

In the qualitative evaluation, we analyzed the WRF behavior from the predicted data with the observed data through time series, in order to show the ability of WRF to represent the time course and the horizontal temperature distribution in RMRJ. The following statistical indices were calculated: correlation coefficient, Normalized Mean Squared Error, Mean Absolute Error and Bias (EEA 2011). In both analyzes, the variable temperature was used two meters from the earth's surface.

Simulated Results and Discussion

To characterize the synoptic condition of the period from January 20th to January 26th, 2014, 2 different maps were prepared: one containing the pressure field to the mean sea level (solid lines), along with the wind at 850 hPa (vector), and another with the geopotential height at 500 hPa, presented in geopotential meter unit. The first map indicates the movement in the atmosphere at low levels (Figures 3a, b), while the second map represents flow at medium levels (Figures 4a, b) as well as an indication of upward/subsident movement of the air. It is noteworthy that the fields of the study period will be compared to the average climatological field prepared with ERA-Interim reanalysis data for the months of January from 1981 to 2010, in order to characterize a possible change in synoptic behavior that favors the increase of temperatures in the city of Rio de Janeiro, during the study period. Reanalysis data are constantly used in climatological studies in order to obtain the behavior of meteorological variables, with a good spatial and temporal resolution. A reanalysis system consists of the combination of an atmospheric model of weather forecasting and data assimilation system. As the observations have an uneven distribution in space and time, assimilation combines such available information to a prediction model to generate a new analysis of weather conditions in certain moments of time. The ERA-Interim project was developed to improve some key aspects of reanalysis ERA40, such as the representation of the hydrological cycle, the quality of the stratospheric circulation and the treatment of deviations and changes in the observation system (Dee and Uppala 2009; Dee et al. 2011; Simmons et al 2006).

Analyzing the pressure field to the mean sea level and wind at 850 hPa, it is observed that the anti-clockwise circulation of the Subtropical

RA Journal of Applied Research
ISSN (e): 2394-6709
||Volume||3||Issue||12||Pages-1270-1287||December-2017||
Index Copernicus ICV: 74.25, DOI: 10.18535/rajar/v3i12.04

Anticyclone of the South Atlantic (SASA) is slightly moved into the South American continent (Figure 3a) compared to its climatological position in January (Figure 3b). This observation is evidenced by isoline of 1016 hPa, whose center is at 25° S - 20°W, from January 20 to 26, 2014, while its climatological position is southeast, centered at 30° S - 10W. Such configuration indicates that there was a predominance of SASA on the state of Rio de Janeiro during the analysis period. Such phenomenon, acting for consecutive days on a particular region may favor the configuration of an atmospheric blocking, which inhibits the incursion of frontal systems and contributes to rising temperatures.

CPTEC/INPE (2014) stressed that, throughout the month of January 2014, no cold front hit the city of Rio de Janeiro. Such condition favors the continued warming of the surface over the days. However, even if the cold fronts have been oceanic, the high-pressure front post system can influence the weather conditions on the continent, acting as a mechanism of decrease in temperature through advection and cold air.

In order to better understand the potential incursion of colder air masses in the region, one can use the geopotential height field at 500 hPa. The highest values of this variable represent a more expanded (heated) troposphere and lower values indicate a colder region. Furthermore, when there is an anti-cyclonic flow in surface, along with high geopotential height values, the vertical movements in the atmosphere become subsidence, which inhibits the formation of clouds and also contributes to a greater surface heating.

It is observed that the climatology of geopotential height in January has a ripple on the Southeast region of Brazil (Figure 4b). Such ripple, however, did not occur in the period from January 20th to 26th, 2014, favoring the configuration of a high geopotencial with 5800 mgp values to the east of the Southeast region, as shown in Figure 4a. During this period, the surface of the anticyclone extends to the middle levels of the atmosphere.

The positioning of SASA, along with the geopotential height field at 500 hPa, are an anticiclonic movement pattern similar to an atmospheric blocking, which inhibits cloud formation and induces the occurrence of high temperatures near the surface (Kunkel et al. 1996; Xoplaki et al. 2003; Meehl and Tebaldi 2004; Palecki et al. 2011).

However, for an actual atmospheric blocking, such configuration must be maintained for a few consecutive days. Therefore, this phenomenon is commonly associated with the occurrence of long episodes of high temperatures (Cassou and Terray 2005; Fischer et al. 2007; Schubert et al. 2011).

Thus, the scenario observed between January 20th and January 26th, 2014 is favorable to the occurrence of HW in the State of Rio de Janeiro, with temperatures rising over the period due to higher incidence of solar radiation on the surface and hence higher heat transfer to the atmosphere.

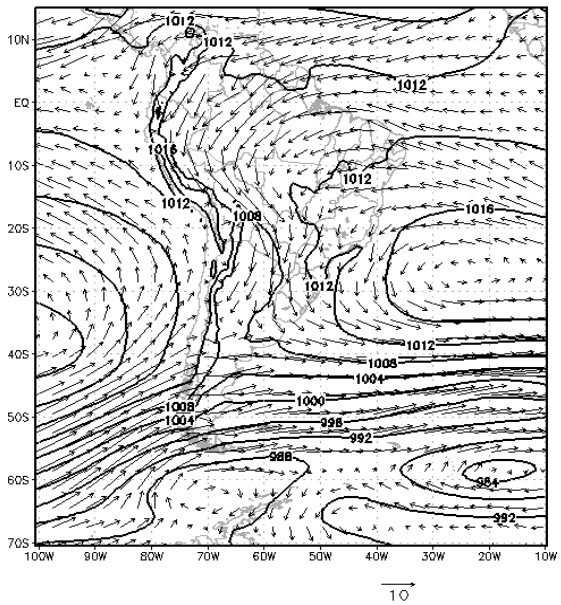

Fig. 3 (a). Average field from 01/20/2014 to 01/26/2014 of the Pressure to the Mean Sea Level (hPa - solid line) and wind at 850 hPa (m/s - vector).

RA Journal of Applied Research
ISSN (e): 2394-6709
||Volume||3||Issue||12||Pages-1270-1287||December-2017||
Index Copernicus ICV: 74.25, DOI: 10.18535/rajar/v3i12.04

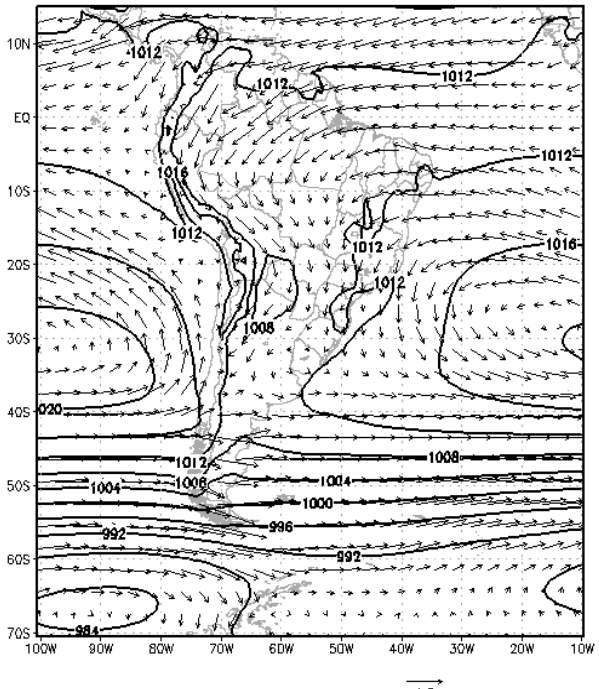

Fig. 3 (b). Climatological average of January between 1981 and 2010 of the Pressure at the Mean Sea Level (hPa - solid line) and wind at 850 hPa (m / s - vector).

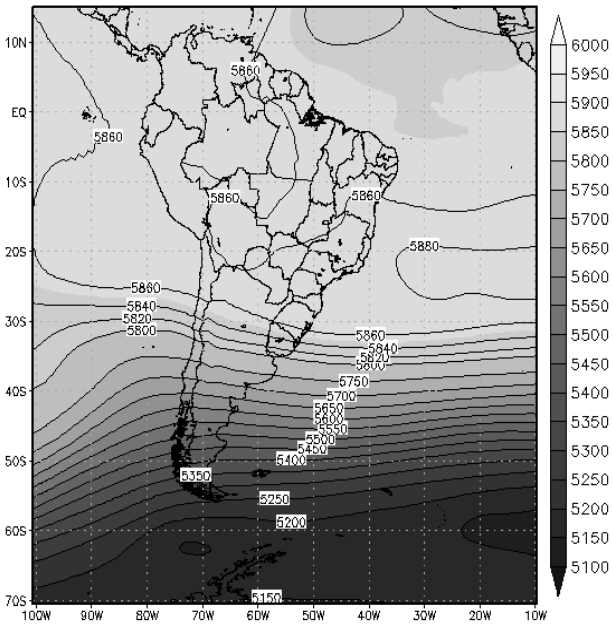

Fig. 4 (a). Average field from 01/20/2014 to 01/26/2014 of the Geopotential Height (mgp) at 500 hPa.

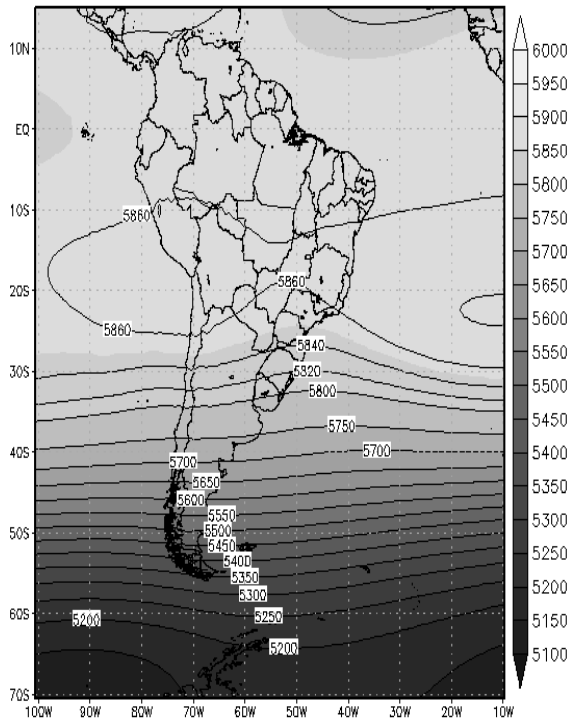

Fig. 4 (b). Climatological average of January between 1981 and 2010 of the Geopotential Height (mgp) at 500 hPa.

Statistical analysis of the modeling results with WRF for the period from 01.20.2014 to 01.26.2014

The analysis highlighted in Table 4 shows that the lower correlation coefficient (R) between the predicted and observed data occurred in airfield SBJR (0.66), and for the remaining stations correlation values greater than 0,85 were obtained, indicating a significant correlation between the behavior of the predicted temperature and the observed data.

The normalized mean square error (EQMN) indicated better results in stations SBGL (0.00) and SBRJ (0.00), with discrepancies in the observed data, not exceeding 10% (0.01). In station SBJR, the value of 0.02 is the most distant from the ideal (0.00). With respect to mean absolute error (MAE), best results were observed in SBGL (0.96°C) and SBRJ (1.57°C) while the major error occurred in SBJR (3.79°C), as seen in the rates of R and EQMN.

RA Journal of Applied Research
ISSN (e): 2394-6709
||Volume||3||Issue||12||Pages-1270-1287||December-2017||
Index Copernicus ICV: 74.25, DOI: 10.18535/rajar/v3i12.04

The BIAS index, in general, showed a tendency to underestimate the simulated data in the study period, except for SBAF, where, on average, forecasts slightly overestimated the observed data (-0.05°C). In SBJR, following the trend of other indexes, the average difference between the predicted and observed data was the most distant from the ideal (3.48°C).

Table 4. Statistical analysis of the air temperature at 2 meters from surface, simulated by the WRF model and the data observed in weather stations of REDEMET and INMET in the studied periods.

Stations / Indexes	R	EQM	MA	BIAS
SBGL	0.94	0.00	0.96	0.15
SBRJ	0.86	0.00	1.57	0.76
SBAF	0.86	0.01	1.97	-0.05
SBJR	0.66	0.02	3.79	3.48
SBSC	0.93	0.01	1.82	1.51

Comparison of WRF and METAR data for the daily temperature cycle

Based on the heat index adopted by Meehl and Tebaldi (2004), in which a heat wave is characterized by a minimum of 5 days with maximum temperature observed 5°C above the normal climatological temperature of the study area, there was a heat wave from January 21st to Janary 25th, 2014. During this period, maximum temperatures greater than 35°C were recorded in most weather stations adopted in this study and a minimum of 5°C difference was obtained compared to the climatology of the maximum temperature of the city of Rio de Janeiro for the month of January, with a value of 30.1°C. The exception occurred in airfield SBJR. Note that the condition for the occurrence of the heat wave in these days of high temperatures was the persistence of synoptic systems acting on the state of Rio de Janeiro, inhibiting cloud formation and achieving greater exposure to solar radiation.

The following review is based on the comparison of the temporal series of variable temperature of the air at 2 meters, from observed data and results of the simulations with WRF model. Figure 5 shows the daily cycles of temperature between January 20th and 26th, 2014, showing that the largest discrepancies between the simulated and recorded results occur in station SBJR. In SBAF and SBSC stations, where the highest temperature ranges are observed, the model underestimated maximum temperatures, while the minimum temperatures were overestimated in SBAF and, finally, in SBSC, there was a good dexterity, with little variation between simulated and observed values. On days when the temperature variations observed were lower, there was a trend towards greater agreement between observed and modeled data, as seen in SBGL airfield in Figure 5 (e). The analysis for SBJR and SBRJ, Figures 5 (c) and (d), is somewhat hampered by the absence of nocturnal observations, but it is possible to verify that the observed maximum temperatures are underestimated by the model in SBJR and there is a good representation of the simulated data with the observed data. Despite some discrepancies in comparison with the observations, the clear signature of the daily cycle of temperature used by the model is remarkable, consistent with the observed data, except for the performance at maximum temperatures of airfield SBJR (Figure 5c), in which there is a tendency to systematically overestimate the observed data.

RA Journal of Applied Research
ISSN (e): 2394-6709
||Volume||3||Issue||12||Pages-1270-1287||December-2017||
Index Copernicus ICV: 74.25, DOI: 10.18535/rajar/v3i12.04

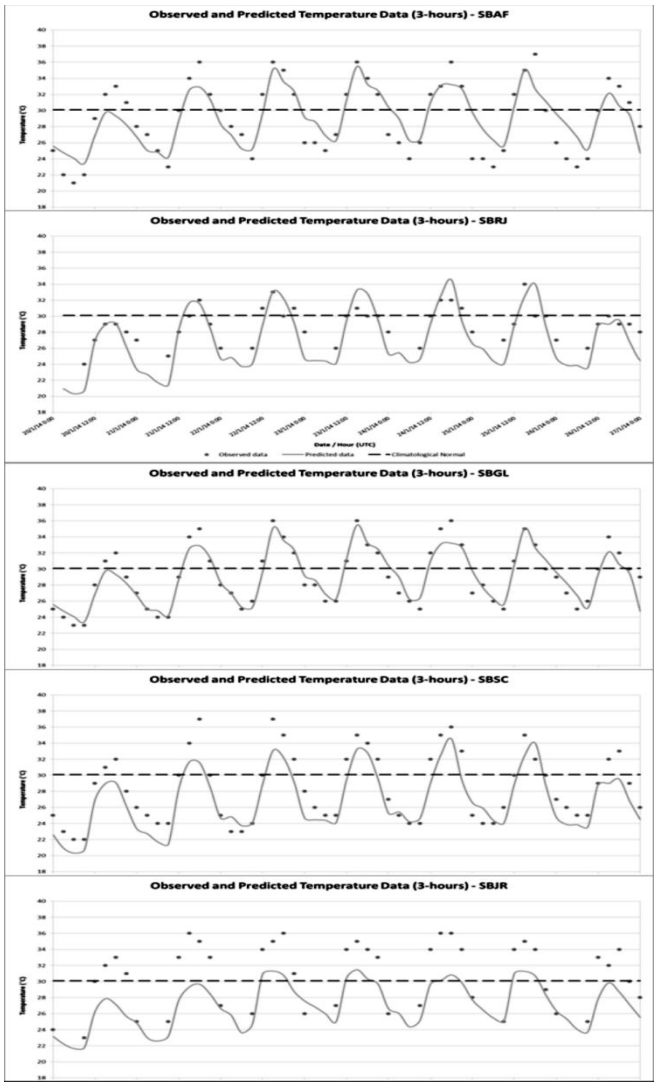

Fig. 5. Temporal evolution of the air temperature in airfields SBAF (A), SBSC (B), SBJR (C), SBRJ (D) and SBGL (E), between January 20th to 26th, 2014. WRF simulations (line) and observed data (dots).

Analysis of horizontal temperature distribution in RMRJ

Figures 6 to 10 show the temperature fields at 2 meters from surface and winds at 10 meters from surface, simulated by WRF model, from January 21st to January 25th, 2014, a period of heat waves in the area of study. The diurnal temperature cycle shows lower temperature amounts at 3 a.m. (Local Time) due to radiative heat loss through the long waves. At that time, temperatures range between 20°C and 26°C, and every day the temperatures in the regions of the North Zone/Centro (Center) of the city of Rio de Janeiro and Baixada Fluminense, both in Air Basin III, are higher than in other regions. At 9 a.m. (local time) there is a more homogeneous temperature distribution due to the beginning of the heating surface, which balances the energy distribution, despite the different types of urban land use as shown in Figure 2 (b). However, lower temperatures are observed in regions of greater topographical elevations (topography in WRF in Figure 2 (c), while in the urban area temperatures reach around 30°C. Both at 3 a.m. and 9 a.m. (local time), the active winds are from the north quadrant, due to the land breeze phenomenon, with moderate intensity in AB I and predominance of light winds in AB II and III, figures 6-10 (a) and (b). In the afternoon, at 3 p.m. (local time) (Figures 6-10 (c)), temperatures remain high due to continued interaction of solar radiation on surfaces with different land uses. At this time, higher temperatures are observed in urban areas of AB I and III. Although there are urbanized areas in Barra da Tijuca, temperatures in AB II region are not as high as in other air basins, as the sea breeze carries a cooler air from the ocean to the mainland, with south wind and, thus, the breeze acts as a cooling mechanism in this region.

Note that the physical processes simulated by the model might not be well represented in the AB II region. Whether due to the energy balance or the cold air advection, discrepancies were found between the simulated and observed temperatures in SBJR, shown in Figure 5 (c). However, WRF represented well the physical processes in SBRJ, since it is also influenced by sea breeze in the afternoon, Figure 5 (d). At 9 p.m. (local time), temperatures decrease due to radiative loss during the night, but even with the decrease in temperature compared to the afternoon, higher temperatures are observed in AB III, due also to

RA Journal of Applied Research
ISSN (e): 2394-6709
||Volume||3||Issue||12||Pages-1270-1287||December-2017||
Index Copernicus ICV: 74.25, DOI: 10.18535/rajar/v3i12.04

the higher heating of this surface in this region throughout the day. Additionally, the sea breeze weakens on the 21st, 23rd and 25th (Figures 6, 8 and 10 (d)), and on the 22nd and 24th the land breeze is already established at 9 p.m. (local time) (Figures 7 and 09 (d)).

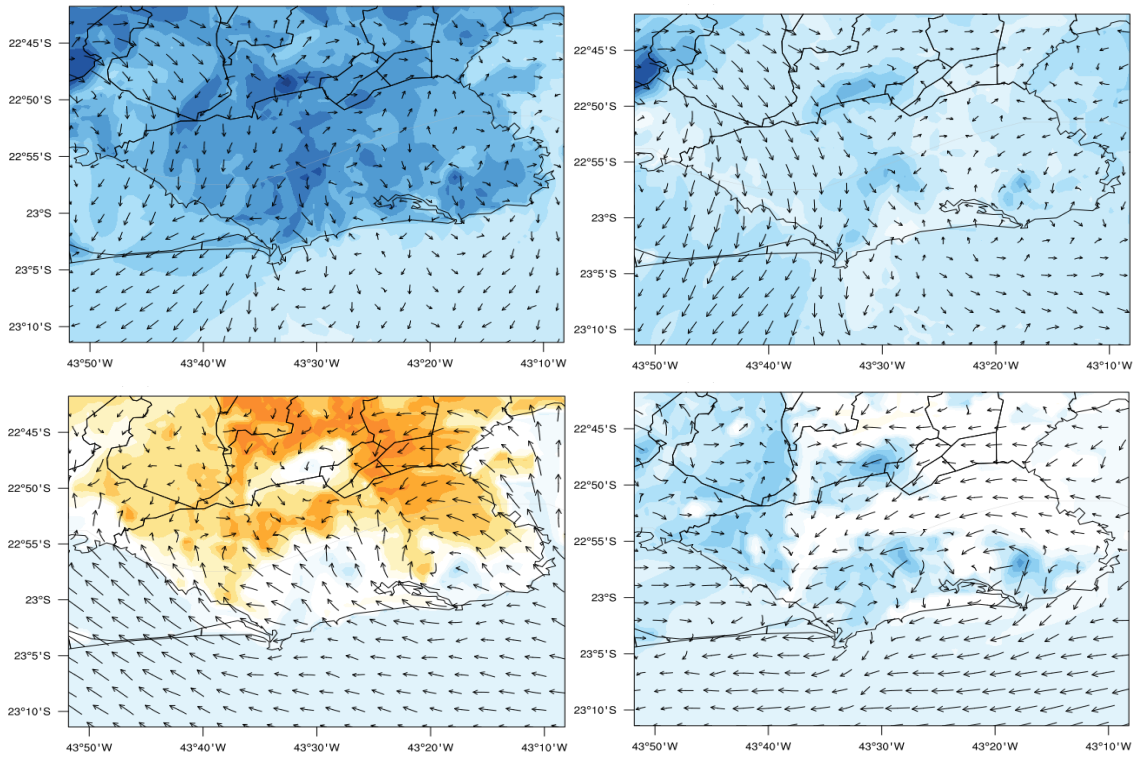

Fig. 6. Air temperature range at 2 meters from surface at 3 a.m. (A), 9 a.m. (B), 3 p.m. (C) and 9 p.m. (D) (local time) on January 21st, 2014, simulated by WRF model.

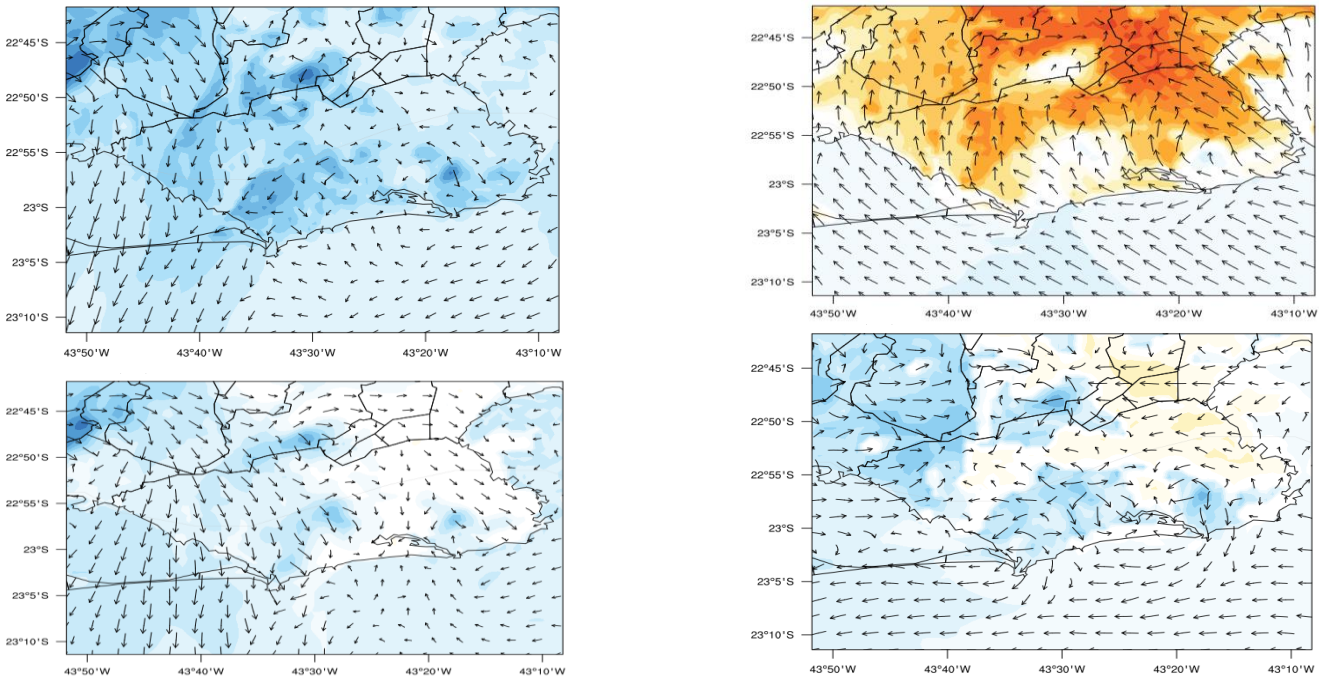

Fig. 7. Air temperature range at 2 meters from surface at 3 a.m. (A), 9 a.m. (B), 3 p.m. (C) and 9 p.m. (D) (local time) on January 22nd, 2014, simulated by WRF model.

RA Journal of Applied Research
ISSN (e): 2394-6709
||Volume||3||Issue||12||Pages-1270-1287||December-2017||
Index Copernicus ICV: 74.25, DOI: 10.18535/rajar/v3i12.04

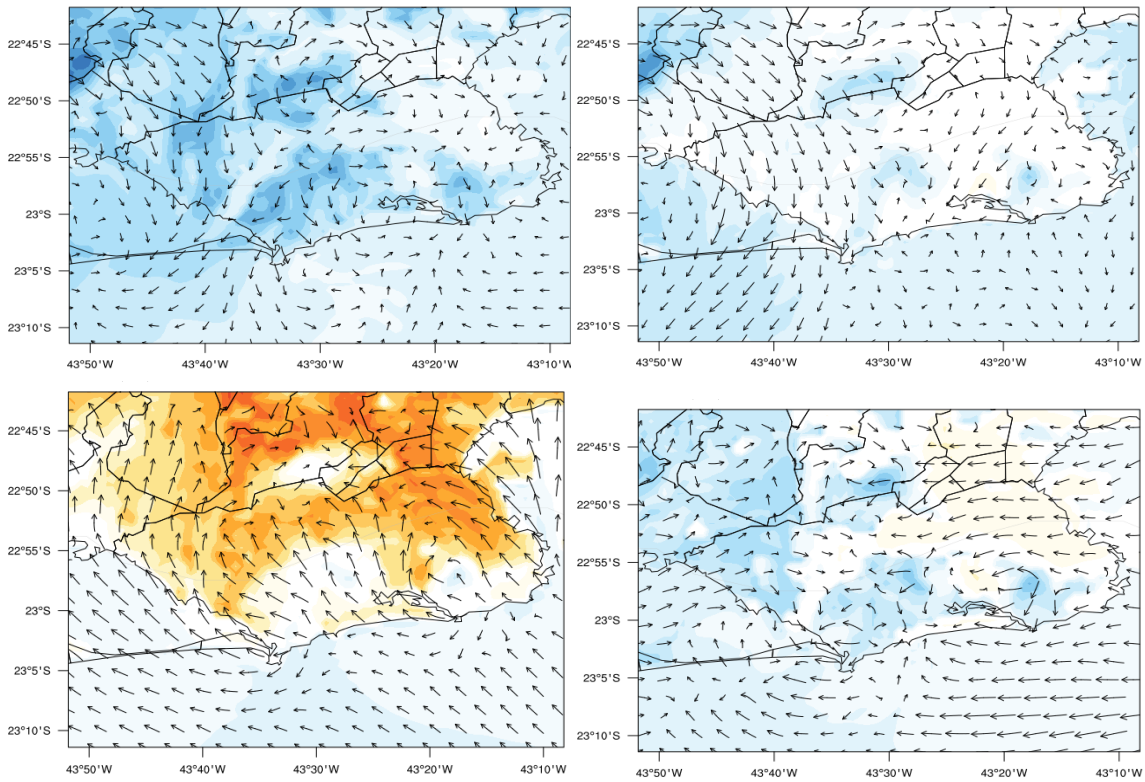

Fig. 8. Air temperature range at 2 meters from surface at 3 a.m. (A), 9 a.m. (B), 3 p.m. (C) and 9 p.m. (D) (local time) on January 23rd, 2014, simulated by WRF model.

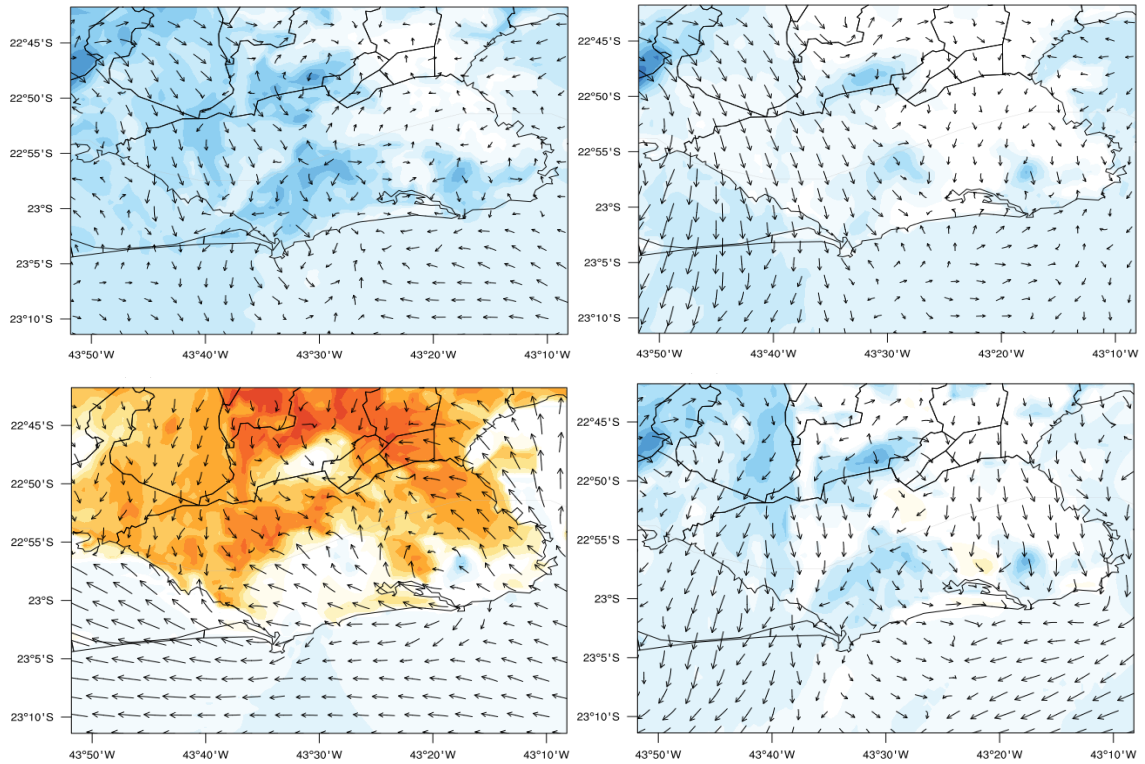

Fig. 9. Air temperature range at 2 meters from surface at 3 a.m. (A), 9 a.m. (B), 3 p.m. (C) and 9 p.m. (D) (local time) on January 24th, 2014, simulated by WRF model.

RA Journal of Applied Research
ISSN (e): 2394-6709
||Volume||3||Issue||12||Pages-1270-1287||December-2017||
Index Copernicus ICV: 74.25, DOI: 10.18535/rajar/v3i12.04

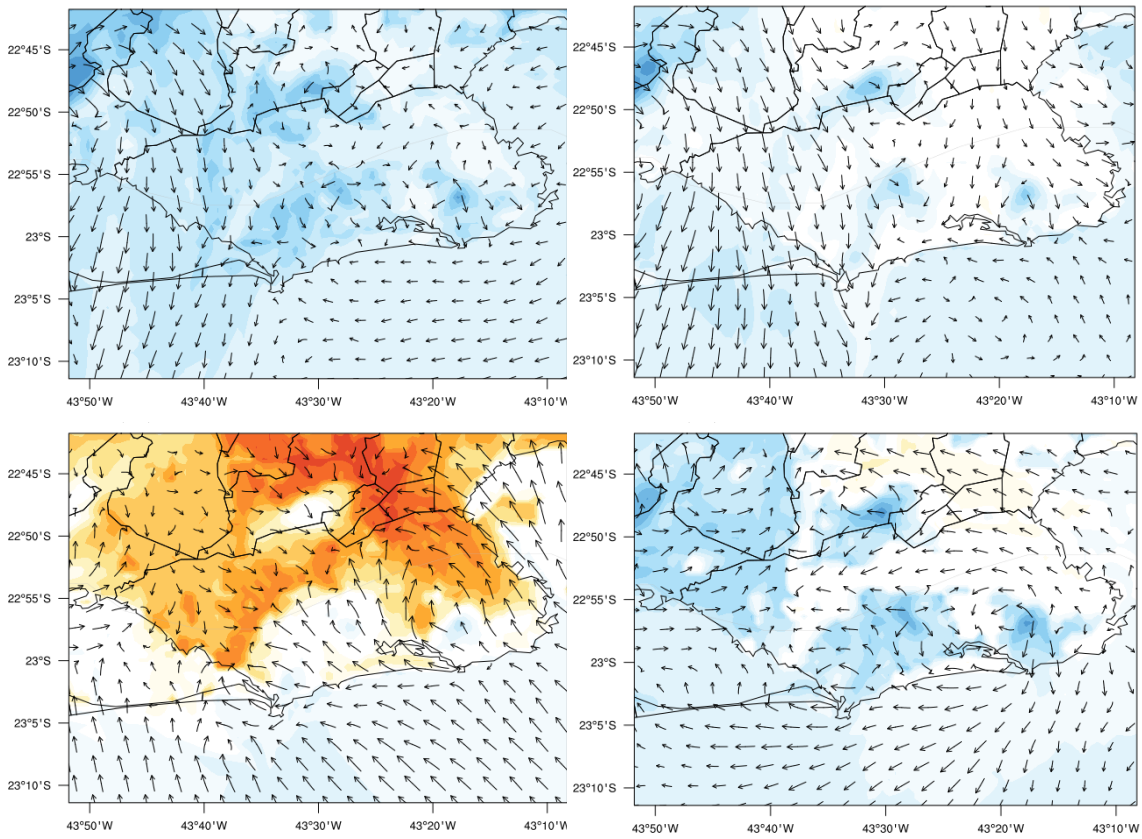

Fig. 10. Air temperature range at 2 meters from surface at 3 a.m. (A), 9 a.m. (B), 3 p.m. (C) and 9 p.m. (D) (local time) on January 25th, 2014, simulated by WRF model.

Conclusions

In this study we observed maximum temperatures rising over the study period, with scenarios of heat waves in Air Basins I, II and III, due to the surface response to the higher incidence of solar radiation as a result of weather setting in synoptic scale of SASA at low levels and high geopotential at average levels of the troposphere.

WRF model adequately reproduced the daily cycle of temperature near the surface and the statistical results showed a slight tendency of the forecasts to underestimate the observed temperatures, with the need for an analysis with a longer period in order to determine a trend of WRF. The analysis of the temporal variation of temperature, combined with the statistical evaluation, indicates that WRF model has the ability in the temporal and spatial distribution of the air temperature at 2 meters from the surface and therefore the heat wave phenomenon in RMRJ, in spite of the discrepancies found in AB II.

A joint analysis of the monitoring of the observed data and atmospheric modeling is a public management tool able to detect the most susceptible areas to heat waves in cities. Thus, the prognostic data from the modeling, along with the knowledge of atmospheric conditions at synoptic and local scale, and the monitoring of meteorological variables contribute to making the right decisions in urban and environmental planning. Whereas the changes in the local climate, due to changes in environmental conditions, cause an impact on city dwellers, the inclusion of climatic factors is vitally important as a source of subsidy to urban planning, where this

RA Journal of Applied Research
ISSN (e): 2394-6709
||Volume||3||Issue||12||Pages-1270-1287||December-2017||
Index Copernicus ICV: 74.25, DOI: 10.18535/rajar/v3i12.04

research emphasized the problem of heat waves in the metropolitan area of Rio de Janeiro.

Acknowledgments

Our sincere thanks to the reviewers and editors for their contributions and acceptance of the article. We are immensely thankful to the PEM (Mechanical Engineering Program), as well as to CAPES (Brazilian Coordination for the Improvement of Higher Education Personnel), which has contributed financially to the performance of the research, and FAPERJ (Research Support Foundation of Rio de Janeiro), important research nourish bodies in Brazil and in the state of Rio de Janeiro.

References

1. Angel, S., Parent, J., Civco, D.L., Blei, A., and Potere, D. (2011). "The dimensions of global urban expansion: estimates and projections for all countries, 2000–2050". *Prog. Plan*. 75, 53–107.
2. Baklanov, A., Molina, L.T., and Gauss, M. (2016). "Megacities, air quality and climate". *Atmospheric Environment* 126, 235 - 249.
3. Bitencourt, D.P., Fuentes, M.V., Maia, P.A., and Amorim, F.T. (2016). "Frequency, Duration, Spatial Coverage, and Intensity of Heat Waves in Brazil". *Revista Brasileira de Meteorologia*, 31(4), 506-517.
4. Cassou, C., Terray, L., and Phillips, A.S. (2005). "Tropical Atlantic influence on European heat waves". *Journal of climate*, 18(15), 2805-2811.
5. Ciais, P., Reichstein, M., Viovy, N., Granier, A., Ogée, J., Allard, V., Aubinet, M., Buchmann, N., Bernhofer, C., Carrara, A., Chevallier, F., De Noblet, N., Friend, A.D., Friedlingstein, P., Grünwald, T., Heinesch, B., Keronen, P., Knohl, A., Krinner, G., Loustau, D., Manca, G., Matteucci, G., Miglietta, F., Ourcival, J.M., Papale, D., Pilegaard, K., Rambal, S., Seufert, G., Soussana, J.F., Sanz, M.J., Schulze, E.D., Vesala, T., and Valentini, R. (2005). "Europe-wide reduction in the primary productivity caused by the heat and drought in 2003". *Nature*. 437, 529–533.
6. Chagas, G.M. (2015). "O processo de reestruturação territorial-produtiva no Extremo Oeste Metropolitano Fluminense: O caso de Itaguaí". Monografia (Graduação em Geografia), Departamento de Geociências, UFRRJ – *Universidade Federal Rural do Rio de Janeiro*.
7. Chemel, C., and Shoki, R.S. (2012). "Response of London's Urban Heat Island to a Marine Air Intrusion in an Easterly Wind Regime". *Boundary-Layer Meteorol*, 144: 65-81.
8. Chen, F. and Dudhia, J. (2001a). "Coupling an advanced land surface-hydrology model with the Penn State-NCAR MM5 modeling system. Part I: Model implementation and sensitivity". *Monthly Weather Review*, 129: 569-585.
9. Chen, F., and Dudhia, J. (2001b). "Coupling an advanced land surface–hydrology model with the Penn State–NCAR MM5 modeling system. Part II: Preliminary model validation". *Monthly Weather Review*, 129(4), 587-604.
10. Chen, F., Kusaka, H., Bornstein, R., Ching, J., Grimmond, C.S.B., Grossman-Clarke, S., Loridan, T., Manning, K.W., Martilli, A., Miao, S., Sailor, D., Salamanca, F.P., Taha, H., Tewari, M., Wang, X., Wyszogrodzki, A.A., and Zhang, C. (2011). "The integrated WRF/urban modeling system:

RA Journal of Applied Research
ISSN (e): 2394-6709
||Volume||3||Issue||12||Pages-1270-1287||December-2017||
Index Copernicus ICV: 74.25, DOI: 10.18535/rajar/v3i12.04

development, evaluation, and applications to urban environmental problems. *International Journal of Climatology*, 31, (2) 273-288.

11. Chen, F., Yang, X.C., and Zhu, W.Q. (2014). "WRF simulations of urban heat island under hot weather synoptic conditions: the case study of Hangzhou City, China". *Atmos. Res.* 138, 364–377.
12. Cleugh, H., and Grimmond, S. (2012). "Urban climates and global climate change". In: Henderson-Sellers, A., McGuffie, Kendal (Eds.), Chapter 3 of *"The Future of the World's Climate"*. Elsevier B.V., ISBN 978-0-12-386917-3.
13. Conti, S., Meli, P., Minelli, G., Solimini, R., Toccaceli, V., Vichi, M., Beltrano, C., and Perini. L. (2005). "Epidemiologic study of mortality during the Summer 2003 heat wave in Italy". *Environmental Research*, v. 98, n. 3, p. 390-399.
14. CPTEC/INPE (Centro de Previsão de Tempo e Estudos Climáticos/ Instituto Nacional de Pesquisas Espaciais). (2014). Climanálise: Boletim de Monitoramento e Análise Climática. V.29, n.1.
15. Dandou, A., Tombrou, M., and Soulakellis, N. (2009). "The influence of the city of Athens on the evolution of the sea-breeze front". *Boundary-Layer Meteorology* 131, 35-51.
16. Dee, D.P., and Uppala, S. (2009). "Variational bias correction of satellite radiance data in the ERA-Interim reanalysis". *Quarterly Journal of the Royal Meteorological Society*, 135(644), 1830-1841.
17. Dee, D.P., Uppala, S.M., Simmons, A.J., Berrisford, P., Poli, P., Kobayashi, S., Andrae, U., Balmaseda, M.A., Balsamo, G., Bauer, P., Bechtold, P., Beljaars, A.C.M., van de Berg, L., Bidlot, J., Bormann, N., Delsol, C., Dragani, R., Fuentes, M., Geer, A.J., Haimberger, L., Healy, S.B., Hersbach, H., H+¦lm, E.V., Isaksen, L., K+Ñllberg, P., K+Âhler, M., Matricardi, M., McNally, A.P., Monge-Sanz, B.M., Morcrette, J.J., Park, B.K., Peubey, C., de Rosnay, P., Tavolato, C., Thepaut, J.N., and Vitart, F. (2011). "The ERA-Interim reanalysis: configuration and performance of the data assimilation system". *Quarterly Journal of the Royal Meteorological Society*, 137, (656) 553-597.
18. EEA (European Environment Agency). (2011). "The application of models under the European Union's Air Quality Directive: A technical reference guide". EEA Technical report No 10/2011. ISSN 1725-2237.
19. Fink, A.H., Brücher, T., Krüger, A., Leckebusch, G.C., Pinto, J.G., and Ulbrich, U. (2004). "The 2003 European summer heatwaves and drought–synoptic diagnosis and impacts". *Weather*, 59 (8), 209-216.
20. Fischer, E.M., Seneviratne, S.I., Lüthi, D., and Schär, C. (2007). "Contribution of land-atmosphere coupling to recent European summer heat waves". *Geophysical Research Letters*, 34(6).
21. Gasparrini, A., and Armstrong, B. (2011). "The impact of heat waves on mortality". *Epidemiology*, v. 22, n. 1, p. 68-73.
22. Grimm, N.B., Faeth, S.H., Golubiewski, N.E., Redman, C.L., Wu, J., Bai, X., and Briggs, J.M. (2008). "Global change and the ecology of cities". *Science*, 319 (5864), 756-760.
23. Hess, J.J., Saha, S., and Luber, G. (2014). "Summertime acute heat illness in U.S.

RA Journal of Applied Research
ISSN (e): 2394-6709
||Volume||3||Issue||12||Pages-1270-1287||December-2017||
Index Copernicus ICV: 74.25, DOI: 10.18535/rajar/v3i12.04

emergency departments from 2006 through 2010: analysis of a nationally representative sample". *Environmental Health Perspectives*, v. 122, n. 11, p. 1209-1215.

24. Hoshiko, S., English, P., Smith, D., and Trent, R. (2010). "A simple method for estimating excess mortality due to heat waves, as applied to the 2006 California heat wave". *International Journal of Public Health*, v. 55, n. 2, p. 133-137.
25. Huang, W., Kan, H., and Kovats, S. (2010). The impact of the 2003 heat wave on mortality in Shanghai, China. *Science of the Total Environment*, v. 408, n. 11, p. 2418–2420.
26. IBGE (Instituto Brasileiro de Geografia e Estatística). (2016). Estimativas de população. Available in http://www.ibge.gov.br/home/estatistica/populacao/estimativa2016/.
27. Jongsik, H., and Kim, H. (2012). "Changes in the association between summer temperature and mortality in Seoul, South Korea". *International Journal of Biometeorology*, v. 57, n. 4, p. 535-544.
28. Kunkel, K.E., Changnon, S.A., Reinke, B.C., and Arritt, R.W. (1996). "The July 1995 heat wave in the Midwest: A climatic perspective and critical weather factors". *Bulletin of the American Meteorological Society*, 77(7), 1507-1518.
29. Kusaka, H., Chen, F., Tewari, M., Dudhia, J., Gill, D.O., Duda, M.G., Wang, W., and Miya, Y. (2012). "Numerical Simulation of Urban Heat Island Effect by the WRF Model with 4-km Grid Increment: An Inter-Comparison Study between the Urban Canopy Model and Slab Model". *Journal of the Meteorological Society of Japan*, 90B: 33-45.
30. Li, D., and Bou-Zeid, E. (2013). "Synergistic interactions between urban heat islands and heat waves: the impact in cities is larger than the sum of its parts". *J. Appl. Meteorol. Climatol*. 52, 2051–2064.
31. Lim, Y.H., Kim, H., and Hong, Y.C. (2012). "Variation in mortality of ischemic and hemorrhagic strokes in relation to high temperature". *International Journal of Biometeorology*, v. 57, n. 1, p. 145-153.
32. Lin, C. Y., Chen, F., Huang, J. C., Chen, W. C., Liou, Y. A., Chen, W. N., and Liu, S.C. (2008). "Urban heat island effect and its impact on boundary layer development and land–sea circulation over northern Taiwan". *Atmospheric Environment*, 42(22), 5635-5649.
33. Meehl, G.A., and Tebaldi, C. (2004). "More intense, more frequent, and longer lasting heat waves in the 21st century". *Science*, 305 (5686), 994-997.
34. Miao, S., Chen, F., LeMone, M., Tewari, M., Li, Q., and Wang, Y. (2009). "An observational and modeling study of characteristics of urban heat island and boundary layer structures in Beijing". *J. Appl. Meteorol. Climatol.*, 48 (3), pp. 484–501.
35. Monteiro, A., Carvalho, V., Oliveira, T., and Souza, C. (2012). "Excess mortality and morbidity during the July 2006 heat wave in Porto, Portugal". *International Journal of Biometeorology*, v. 57, n. 1, p. 155-167.
36. Moraes, N.O., Marton, E., and Pimentel, L.C.G. (2014). "Análise do Desempenho dos Modelos MM5 e WRF na Simulação da Temperatura do Ar em Superfície na RMRJ". *Anuário do Instituto de Geociências*, 37(2), 161-168.

RA Journal of Applied Research
ISSN (e): 2394-6709
||Volume||3||Issue||12||Pages-1270-1287||December-2017||
Index Copernicus ICV: 74.25, DOI: 10.18535/rajar/v3i12.04

37. Ostro, B.D., Roth, L.A., Green, R.S., and Basu, R. (2009). "Estimating the mortality effect of the July 2006 California heat wave". *Environmental Research*, v. 109, n. 5, p. 614-619.
38. Paiva, L.M.S., Bodstein, G.C.R., and Pimentel, L.C.G. (2014). "Influence of high-resolution surface databases on the modeling of local atmospheric circulation systems". *Geoscientific Model Development*, 7(4), 1641-1659.
39. Palecki, M.A., and Groisman, P.Y. (2011). "Observing climate at high elevations using United States Climate Reference Network approaches". *Journal of Hydrometeorology*, 12(5), 1137-1143.
40. Quattrochi, D.A., and Luvall, J.C. (1997). "Application of high-resolution thermal infrared remote sensing and GIS to assess the urban heat island effect". *Int. J. Remote Sens.* 18, 287–304.
41. Rizwan, A.M., Dennis, Y.C.L., and Liu, C. (2008). "A review on the generation, determination and mitigation of Urban Heat Island". *J. Environ. Sci*. 20, 120–128.
42. Salamanca, F., Martilli, A., and Yagüe, C. (2012). "A numerical study of the Urban Heat Island over Madrid during the DESIREX (2008) campaign with WRF and an evaluation of simple mitigation strategies". *International Journal of Climatology*, 32: 2372–2386.
43. Schubert S.D., Wang H., and Suarez M.J. (2011). "Warm season subseasonal variability and climate extremes in the Northern Hemisphere: the role of stationary Rossby waves". *J. Clim*. 24(18): 4773–4792.
44. Semenza, J.C., Rubin, C.H., Falter, K.H., Selanikio, J.D., Flanders, W.D., Howe, H.L., and Wilhelm, J.L. (1996). "Heat-Related deaths during the July 1995 heat wave in Chicago". *The New England Journal of Medicine*, v. 335, n. 2, p. 84-90.
45. Seto, K.C., Güneralp, B., and Hutyra, L.R. (2012). "Global forecasts of urban expansion to 2030 and direct impacts on biodiversity and carbon pools". *Proc. Natl. Acad. Sci*. 109, 16083–16088.
46. Shafran, P.C., Seaman, N.L., and Gayno, G.A. (2000). "Evaluation of numerical predictions of boundary layer structure during the Lake Michigan Ozone Study". *J. Appl. Meteor.*, 39, 412–426.
47. Simmons, A., Uppala. S., Dee, D., and Kobayashi, S. (2006). "ERA-Interim: New ECMWF reanalysis products from 1989 onwards". *ECMWF Newsletter*, 110: 25-35
48. Skamarock, W.C., Klemp J.B., Dudhia, J., Gill, D.O., Barker. D.M., Duda, M.G., Huang, X.Y., Wang, W., and Powers, J.G. (2008). "A Description of the Advanced Research WRF Version 3: NCAR Technical Note TN–475+ STR". National Center for Atmospheric Research Boulder, Colorado, USA.
49. Stéfanon, M., Drobinski, P., D'Andrea, F., Lebeaupin-Brossier, C., and Bastin, S. (2014). "Soil moisture-temperature feedbacks at meso-scale during summer heat waves over Western Europe". *Climate dynamics*, 42(5-6), 1309-1324.
50. Tasian, G.E., Pulido, J.E., Gasparrini, A., Saigal, C.S., Horton, B.P., Landis, J.R., Madison, R., and Keren, R. (2014). "Daily mean temperature and clinical kidney stone presentation in five U.S. metropolitan areas: A time-series analysis". *Environmental Health Perspectives*, v. 122, n. 10, p. 1081-1087.
51. United Nations. (2014). Department of Economic and Social Affairs, Population

RA Journal of Applied Research
ISSN (e): 2394-6709
||Volume||3||Issue||12||Pages-1270-1287||December-2017||
Index Copernicus ICV: 74.25, DOI: 10.18535/rajar/v3i12.04

Division. "World urbanization prospects: The 2014 revision". New York: NY, United Nations 2014.

52. Vautard, R., Honore, C., Beekmann, M., & Rouil, L. (2005). "Simulation of ozone during the August 2003 heat wave and emission control scenarios". *Atmospheric Environment*, 39(16), 2957-2967.
53. Xoplaki, E., Gonzalez-Rouco, J.F., Luterbacher, J., Wanner, H. (2003). Mediterranean summer air temperature variability and its connection to the large-scale atmospheric circulation and SSTs. *Clim Dyn*. 20: 723–739.